Defined medium conditions for the induction and expansion of human pluripotent stem cell-derived retinal pigment epithelium.

Grace E. Lidgerwood[1], Shiang Y. Lim[2], Duncan E. Crombie[1], Ray Ali[3], Katherine P. Gill[1], Damián Hernández[2], Josh Kie[4], Alison Conquest[1], Hayley S. Waugh[1], Raymond C.B. Wong[1], Helena H. Liang[1], Alex W. Hewitt[1, 3*], Kathryn C. Davidson[1,&,*] and Alice Pébay[1, * ^]

[1] *Centre for Eye Research Australia, Royal Victorian Eye and Ear Hospital & Department of Ophthalmology, the University of Melbourne, East Melbourne, Victoria, Australia*

[2] *O'Brien Institute Department, St Vincent's Institute of Medical Research, Fitzroy, Victoria, Australia.*

[3] *School of Medicine, Menzies Institute for Medical Research, University of Tasmania, Tasmania, Australia*

[4] *Department of Anatomy and Neuroscience, University of Melbourne, Parkville, Victoria, Australia*

[*] Co-senior authors

[&] *Current address: Australian Regenerative Medicine Institute, Monash University, Clayton, Victoria, Australia*

Running Title: human pluripotent stem cell differentiation in RPE

Author contributions. K.P.G., R.A., S.Y.L., D.H., A.C., D.E.C., H.S.W., R.C.B.W., H.H.L., J.K., A.W.H.: collection and/or assembly of data, data analysis and interpretation, final

approval of manuscript. G.L., K.D., A.P.: concept and design, financial support, data analysis and interpretation, manuscript writing, final approval of manuscript.

^ Corresponding author: Alice Pébay, PhD

Address: CERA, University of Melbourne, 32 Gisborne Street, East Melbourne, VIC 3002, Australia. Phone: +61 3 99298165. Fax: +61 3 9662 3859. Email: apebay@unimelb.edu.au

Keywords. Human induced pluripotent stem cells; human embryonic stem cells; retinal pigment epithelium, differentiation, RNA sequencing, electrophysiology.

Summary

We demonstrate that a combination of Noggin, Dickkopf-1, Insulin Growth Factor 1 and basic Fibroblast Growth Factor, promotes the differentiation of human pluripotent stem cells into retinal pigment epithelium (RPE) cells. We describe an efficient one-step approach that allows the generation of RPE cells from both human embryonic stem cells and human induced pluripotent stem cells within 40-60 days without the need for manual excision, floating aggregates or imbedded cysts. Compared to methods that rely on spontaneous differentiation, our protocol results in faster differentiation into RPE cells. This pro-retinal culture medium promotes the growth of functional RPE cells that exhibit key characteristics of the RPE including pigmentation, polygonal morphology, expression of mature RPE markers, electrophysiological membrane potential and the ability to phagocytose photoreceptor outer segments. This protocol can be adapted for feeder, feeder-free and serum-free conditions. This method thereby provides a rapid and simplified production of RPE cells for downstream applications such as disease modelling and drug screening.

Introduction

Retinal degenerative diseases such as age-related macular degeneration (AMD) and other retinopathies lead to the impairment or degeneration of photoreceptor cells, ultimately leading to irreversible vision loss or blindness. Loss of the RPE, either as a primary or secondary event, is common and there are currently no direct means to halt RPE death once photoreceptors have degenerated. This highlights the pressing need to generate functional RPE cells *in vitro*, not only to improve outcomes of retinal diseases through disease modelling and drug screening, but also as a potential source of tissue for cell replacement therapies [1]. Human pluripotent stem cells (hPSCs), including human embryonic stem cells (hESCs) and induced pluripotent stem cells (iPSCs), have generated great expectations in the field of regenerative medicine due to their ability to propagate indefinitely *in vitro* and to give rise to any cell type in the body. Human iPSCs in particular may be used to generate patient-specific cells for autologous cell transplantation [2] and were recently approved for transplantation of iPSC-derived RPE cells in a clinical trial in human patients in Japan [3]. Furthermore, hESC-derived RPE cells safely integrate in the human eye following submacular transplantation and are currently in phase I/IIa clinical trials in humans for Stargardt disease and AMD [4, 5]. Together, these highlight the potential of hPSC-derived RPE cells in therapeutics for patients suffering a range of retinal conditions.

A variety of protocols have been described to differentiate hPSCs into RPE cells which involve varying degrees of complexity and efficiency (reviewed in [6]). hPSCs can spontaneously differentiate into a heterogeneous population of cells, which often includes RPE cells, if cultured at high density for extended periods of time and/or in suspension as embryoid bodies [7]. However, spontaneous differentiation methods to generate RPE can be

inefficient, lengthy, around 6 months, highly variable between cell lines, and rely on accurate excision of pigmented foci from mixed cultures [8-12]. More efficient methods for obtaining and propagating RPE cells consist of guided and sequential differentiation of hPSCs towards RPE cells using combinations of growth factors and/or small molecules, such as basic Fibroblast Growth Factor (bFGF), the Bone Morphogenetic Protein (BMP) antagonist Noggin, the Wnt antagonist Dickkopf-1 (DKK1) or its agonist CHIR99021, nicotinamide, casein kinase I inhibitor 7, the ALK4 inhibitor SB-431542 and the Rho-associated kinase inhibitor Y-27632 [8, 13-17]. A three-dimensional differentiation approach can also be used, with formation of cysts or eye cup structures in defined medium, prior to RPE enrichment [15, 18-20]. Although these protocols use a directed approach to produce functional RPE cells, they are complex.

Lamba *et al.* demonstrated that the combination of bFGF, Noggin, DKK1, Insulin Growth Factor (IGF) -1, B27 and N2 supplements promoted differentiation of hESC-derived embryoid bodies towards retinal progenitor cells able to generate retinal neurons [21, 22]. Here, we assessed whether these factors could also promote differentiation of hPSCs towards RPE when delivered with additional medium components optimized for RPE cells found in the RPE-enrichment basal medium (RPEM) [23]. We found this combination of growth factors enables a reproducible and simplified one-step method to generate and propagate RPE cells from hPSCs and is adaptable to feeder-free and serum-free conditions. This protocol also results in faster differentiation of hPSCs into RPE cells compared to timeframe reported in conventional spontaneous differentiation-based methods [7, 9, 24].

Materials and Methods

Ethics. All experimental work performed in this study was approved by the Human Research Ethics committees of the Eye and Ear Hospital (11/1031H, 13/1151H-004) and University of Melbourne (0605017, 0829937) with the requirements of the National Health & Medical Research Council of Australia (NHMRC) and conformed with the Declarations of Helsinki.

Maintenance of human PSCs. The iPSC line iPS (Foreskin) 4 clone 2 (ES4CL2) [25] and the hESC line H9 [26] were maintained in Knockout Serum Replacement medium (KSRM) containing DMEM:F-12 with GlutaMAX, 20% Knockout Serum Replacement, 0.1mM Modified Eagles Non-Essential Amino Acids (MEM NEAA), 1% penicillin and streptomycin, 0.1mM β-mercaptoethanol (all from Invitrogen) supplemented with bFGF (10 ng/mL, Millipore) on irradiated CF1-strain mouse embryonic fibroblast feeders (feeder cultures) with weekly passages using dispase (Sigma-Aldrich) for maintenance. In some experiments, hPSCs were cultivated in a feeder-free system using Vitronectin XF™ (Stem Cell Technologies) in serum-free complete medium TeSR™-E8™ (Stem Cell Technologies) and maintained by passaging with ReLSR (Stem Cell Technologies) once a week.

RPE cell differentiation. When hPSC colonies reached confluence (day 0, Fig. 1), medium was replaced with RPEM containing α-MEM, 5% foetal bovine serum (FBS), 0.1mM MEM NEAA, 0.1mM N2 supplement, 1% L-Glutamine–Penicillin–Streptomycin solution, 250 μg/mL Taurine, 20 ng/mL Hydrocortisone and 13pg/mL Triiodothyronine (all from Sigma-Aldrich), adapted from [23] (Fig. 1). In some experiments, serum-free RPEM (SF-RPEM) was used, supplemented 25 mM HEPES in place of the serum (Fig. 1). Both RPEM were

further supplemented with IGF1 (10 ng/mL, Peprotech), Dkk1 (10 ng/mL, Peprotech), Noggin (10 ng/mL, R&D Systems), bFGF (5 ng/mL), B27 and N2 (both 1x, Invitrogen), which we refer as the growth factor cocktail (GFC; Fig. 1A). Culture medium supplemented with GFC was changed every second day, for up to 60 days or until cells had acquired an RPE-like polygonal morphology and visible pigmentation. Cells were then passaged with a 5 minute exposure to 0.25% Trypsin (Invitrogen) onto Matrigel-coated (BD Biosciences) tissue culture plates at a density of 7.5 x 10^4 cells/cm^2 in 15% FBS- RPEM + GFC overnight, then replaced to RPEM +GFC.

RPE extraction from human post-mortem eyes. Post-mortem eyes were obtained from the Lions Eye Donation Service (LEDS). Eyes were retrieved from donors within 13 hours of death, and RPE tissue collected within 12 - 33 hours of death. Following removal of the cornea, the sclera of the posterior globe was incised in quadrants towards the optic nerve, exposing the choroid sac. Following an incision of the choroid, the iris-lens complex was carefully removed. The vitreous was removed, and the choroid carefully teased from the remaining scleral base. The choroid and retina were gently cut from their attachment at the lamina cribrosa where the optic nerve exits the globe. Following removal of the retina, the choroid and RPE layer were carefully separated under a dissection microscope. RPE tissues were extracted from both the left and right eyes of each donor and pooled together before RNA was extracted using the RNeasy mini kit (Qiagen), following manufacturer instructions. In total, three individual donors were analysed.

Quantitative real-time polymerase chain reaction. Total RNA was isolated using the RNeasy Plus Mini Kit and treated with DNase 1 (all from Qiagen). cDNA was synthesized

from 500-1000 ng of RNA using the High Capacity cDNA Reverse Transcription Kit (Life Technologies). qRT-PCR was performed on a StepOne Plus Real-Time PCR system (Applied Biosystems) in duplicate, 20 μL reactions. The expression levels were normalized to the *GAPDH* housekeeping gene. The following genes were analysed: *NANOG* Hs02387400_g1, *OCT4* Hs00999632_g1, *PAX6* Hs00240871_m1, *SIX3* Hs00193667_m1, *RAX* Hs00429459_m1, *MITF* Hs01117294_m1, *PMEL* Hs00173854_m1, *CRALBP*/*RLBP1* Hs00165632_m1, *RPE65* Hs01071462_m1, and *GAPDH* Hs99999905_m1.

Photoreceptor outer segment (POS) isolation. POS were isolated according to established protocols [27, 28] from 40 bovine eyes fresh from the slaughterhouse. Bovine retina were dissected under dim red light and collected into homogenization buffer (20% sucrose, 20 mM Tris Acetate pH 7.2, 2 mM $MgCl_2$, 10 mM glucose, 5mM taurine). Following collection, the retina suspension was shaken to disrupt the cell layers and filtered three times through sterile gauze to remove large tissue fragments. The resulting crude retina suspension was layered over a chilled 25-60% continuous sucrose gradient in 20mM Tris Acetate pH 7.2, 10 mM glucose, 5 mM taurine [29], then centrifuged at 25,000 rpm for 50 min at 4°C. The POS-containing orange band was collected, washed in 5-volumes of ice-cold Buffer 1 (20 mM Tris Acetate pH 7.2, 5mM taurine), and pelleted by centrifugation at 5,000 rpm for 10min at 4°C. POS were washed next in Buffer 2 (10% sucrose, 20 mM tris acetate pH 7.2, 5 mM taurine), followed by a final wash in Buffer 3 (10% sucrose, 20 mM sodium phosphate pH 7.2, 5 mM taurine). POS were resuspended in DMEM containing 2.5% sucrose, counted on a hemocytometer, aliquoted and stored at -80°C. To label with FITC, POS were resuspended in 10 mL Buffer 3 after the final wash and incubated with 0.4 mg/mL FITC isomer (Life Technologies, prepared as a 2.5 mg/mL stock in 0.1M Na carbonate pH 9.5) for 1.5h at room

temperature with gentle rotation. Labelled POS were washed twice in Buffer 3, then once in DMEM, and resuspended in DMEM with 2.5% sucrose, counted, aliquoted and frozen as described above.

POS phagocytosis assay. Phagocytosis was assessed by flow cytometry following incubation of RPE cells with FITC-labelled POS (FITC-POS) as described in [30], incubating 200,000 FITC-POS/cm^2 with RPE for 5h at 37°C. RPE cells were incubated with 140 ng/mL DAPI and analysed on a Becton Dickinson FACS Aria III flow cytometer. Analysis was performed using FCS Express 5 (DeNovo Software). The percentage of RPE cells that internalized the FITC-POS was measured from the DAPI-negative gated live cell population. This population was initially gated by size (Forward vs Side scatter) to exclude POS.

Immunocytochemistry. Immunocytochemistry was performed using the following primary antibodies: ZO-1 (10 µg/mL, Life Technologies), MITF (1 µg/mL, Abcam), Bestrophin (BEST, 47 µg/mL, Novus), Occludin (OCC, 2 µg/mL, R&D Systems), RPE 65 (10 µg/ml, Abcam), PMEL (5.2 µg/mL, Abcam), CRALBP (10 µg/mL, Abcam). Cells were then immunostained with a species specific secondary antibody (Alexa Fluor 568 or 488, Life Technologies). Nuclei were counter-stained with DAPI (1µg/mL, Invitrogen). Antibody specificity was verified by the absence of staining in an isotype-matched negative control immunoglobulin fraction (Life Technologies). Purity of RPE culture was quantified using ImageJ (NIH) by manually counting ~250 cells per sample stained with PMEL and counterstained with DAPI (P1, 6 independent experiments, n=3 for H9- and n=3 for ES4CL2-derived cells) from pictures randomly taken.

Electrophysiology. Whole-cell patch clamp recording of cells was performed using the Port-a-Patch system with external and internal modules (Nanion Technologies GmbH, Munich, Germany) and the PatchControlHT software (Nanion Technologies) was used for cell capture, seal formation and whole-cell access. The Port-a-Patch uses ECP-10 patch clamp ampliers (HEKA Elektronik, Lambrecht/Pfalz, Germany) and PatchMaster software (HEKA) for data acquisition and analysis. Borosilicate glass NPC-1 chips with low resistance (1-3.5 MOhm) were used for all recordings. Briefly, confluent hPSC-derived RPE cells grown on Matrigel-coated plates were treated with 0.25% Trypsin (Invitrogen) for 10 minutes and inactivated with DMEM supplemented with 10% FBS. Cells were mechanically triturated to ensure a single cell suspension in external solution (140 mM NaCl, 4 mM KCl, 1 mM $MgCl_2$, 2 mM $CaCl_2$, 5 mM D-glucose monohydrate, 10 mM HEPES/NaOH, pH 7.4, 298 mOsmol). The chips were set up with 5 μL of internal solution (50 mM KCl, 10 mM NaCl, 60 mM K-fluoride, 20 mM EGTA, 10 mM HEPES/KOH, pH 7.2, 285 mOsmol) and 5 μL of external solution to create a continuous circuit. Approximately 2500 cells (in 5 μL) were added to the external solution from which a single cell was captured and the software initiated the whole cell patch clamp automatically. The seal resistance was typically 0.5–1.0 GOhm. All experiments were carried out at room temperature (24 °C). A voltage step protocol (20 mV increments) was performed between −100 mV and +40 mV (200 ms duration) for the K^+ channel, and between −100 mV and +20 mV (20 ms duration) for the Na^+ channels. A total of 19 cells were analysed (9 from ES4CL2-derived RPE cells, 10 from H9-derived RPE cells, all at P1).

RNA sequencing. RNA was prepared as previously described from three independent human RPE donors and three H9-derived RPE cells (differentiated in 5%RPEM + GFC on feeder

free system) at day 60 (P0). All samples were DNase treated, rRNA depleted and then analysed on an Illumina HiSeq2000 using 100bp paired-end chemistry at the Australian Genome Research Facility (AGRF; Victoria, Australia). Primary sequence data were generated using the Illumina Consensus Assessment of Sequence And Variation 1.8.4 pipeline. An average of 27M reads were obtained per sample. Expression data are available through the Sequence Read Archive (www.ncbi.nlm.nih.gov/sra) data accession number: SPA####Pending####.

Statistical Analysis. Unless otherwise stated all experiments were performed three independent times in triplicate. Summary statistical analyses were performed in Graphpad Prism software (v5.04, www.graphpad.com). Comparisons between experimented were performed using the unpaired t-test, One-way and Two-way ANOVA with the Tukey's or Sidak multiple comparison test. Statistical significance was established as *$p<0.05$, **$p<0.01$, ***$p<0.001$, ****$p<0.0001$.

The paired-end RNA-seq data were uploaded into a Galaxy instance hosted by the Texas Advanced Computing Centre. FastQC was used to investigate data quality [31]. Residual adapter sequences were removed and low quality read ends trimmed using fixed-length trimming from the FASTX-Toolkit [31]. High quality trimmed sequences were aligned against the hg19 reference genome using the Tophat Gapped-read mapper for RNA-seq data (Galaxy Tool Version 0.9) with default parameters [32]. Transcriptome assembly and transcript abundance estimation was performed using Cufflinks (Galaxy Tool Version 2.2.1.0) strictly using a hg19 GTF annotation with quartile normalisation and bias correction [32]. Variance Stabilizing Transformation was performed using DESeq2 for direct differential gene expression comparisons [33].

Results

Growth factor cocktail mediates differentiation of hPSCs into RPE cells.

Using the protocol described in Fig. 1, two undifferentiated hPSC lines were cultivated in RPEM or SF-RPEM supplemented with Noggin, DKK-1, IGF1, bFGF, B27 and N2, referred as the GFC (Fig. 1A). Pigmentation was observed by day 40 and maximal pigmentation occurred by day 60 (Fig. 1B). At this time, in order to gain a more homogeneous population of RPE, cells were enzymatically passaged and replated onto Matrigel-coated dishes (referred as passage (P) 0: day 60, Fig. 1A). Subsequent passaging was further performed (P1: day 90 and P2: day 120). Cells were assessed for expression of eye field and RPE cell markers and phagocytosis function (Fig. 1).

Within 7 days in RPEM+GFC conditions, notable cell morphology changes were observed for both cell lines cultivated on feeder cells, with cells adopting a polygonal morphology typical of RPE cells (Fig. 1B). By day 20, significant and widespread changes in cell morphology were observed, with a large number of cells exhibiting RPE-like morphology and subtle pigmentation (Fig. 1B). By day 40, the pigmentation was widespread and further intensified (Fig. 1B). Similar data was observed with cells cultivated in RPEM+GFC without feeders. Cells exhibited typical RPE-like morphology and formed fluid-filled bulges known as “blisters”, which may be indicative of functional transport of fluid from the apical to basal surface of cells [24, 34]. Given that the basal medium contained important pro-neural and retinal components such as B27 and N2, taurine, hydrocortisone and triiodothyronine [23, 35-37], we investigated if this alone provided an adequate environment for promoting differentiation to RPE. Unlike in the presence of GFC, little pigmentation was observed in cells receiving basal RPEM alone and qPCR analysis confirmed indicating that

the enhanced differentiation of hPSCs to RPE cells in our protocol is dependent upon GFC (Suppl. Fig. 1).

We examined the gene expression of pluripotent (*NANOG*, *OCT4)*, eye field (*SIX3*, *RAX*, *PAX6*) and mature RPE (*MITF*, *PMEL*, *RPE-65*, *CRALBP*) markers in hPSC-derived cells cultivated on feeders or without, in the presence of GFC after the cells pigmented, (P0, day 60, Fig. 2A). As expected, the GFC-derived RPE cells showed a significant down regulation of pluripotency-associated genes *NANOG* and *OCT4* relative to their respective undifferentiated stem cell controls (Fig. 2A). Expression of the eye field genes *SIX3*, *RAX* and *PAX6* was markedly increased in all hPSC-derived RPE cells (Fig. 2A). Similarly, *MITF* and its downstream target gene *PMEL* were also increased in both H9- and ES4CL2-derived RPE cells (Fig. 2A). Finally, the mature RPE markers *RPE-65* and *CRALBP* were highly upregulated for both lines (Fig. 2A). We observed no significant difference in levels of expression of any of the mature markers (*MITF*, *PMEL*, *CRALBP* or *RPE65*) between hPSC-derived RPE cells and native human RPE cells (Fig. 2A), demonstrating that RPE cells derived using a GFC express appropriate defining markers of mature RPE cells.

Following P1, both hESC- and iPSC-derived pigmented cells stained positive for the more mature RPE markers MITF, OCC, BEST and ZO-1 (Fig. 2B). Expression of these markers was regular across the culture suggesting a homogenous degree of maturity of cells within the culture. Functionality of hPSC-derived RPE cells was also assessed by measuring phagocytosis of FITC labeled bovine photoreceptor outer segments (POS). As shown in Fig. 2C and 2D, >95% of cells obtained by P1 of this protocol were capable of phagocytosis of bovine POS. The P1-hPSC-derived RPE cells also showed functional K^+ transport (Fig. 2E),

similar to that observed in native RPE cells [38]. In all cells, a positive K^+ channel was detected (Fig. 2E). By contrast, no Na^+ current was detected in any of the cells analysed, which indicates that the derived RPE cells do not bear any artifacts of the neural progenitors from which they are derived [39] (Fig. 2E). Together, these data demonstrate the maturity and functionality of RPE cells derived from this protocol.

We next sought to ascertain if the expression of mature markers for RPE was modified upon consecutive passaging of pigmented cells on Matrigel-coated plates and in RPEM medium supplemented with GFC (P1-2; Fig. 2F). RNA was extracted from P0 (day 60), P1 (day 90) and P2 (day 120) RPE cells and analyzed by qRT-PCR for both H9 and ES4CL2 (Fig. 2F, G). A low but detectable level of expression of pluripotent markers *NANOG* and *OCT4* was maintained with each RPE passage, and no significant differences were observed in eye field and RPE gene expression upon passaging (Fig. 2F, G). These data suggest that RPE cells derived from H9 and ES4CL2 reach maturity early in the protocol (within the first 60 days) and are able to maintain that maturity following two subsequent enzymatic passages.

Optimization of RPE differentiation in feeder-free and serum–free conditions.

In order to optimize our protocol to a more defined environment, we applied the GFC-mediated differentiation method to hPSCs cultured in feeder-free and serum-free conditions according to the timeline detailed in Fig. 1. H9 and ES4CL2 were grown to confluence, after which time the medium was transitioned to SF-RPEM with GFC. By day 30, noticeable pigmentation had emerged. qRT-PCR analysis of differentiated cells grown in both media

without feeders at day 60 revealed the downregulation of pluripotency markers *NANOG* and *OCT4,* and an increase in the mRNA expression of early eye field and mature RPE markers (Fig. 3A). In addition, cells cultivated with SF-RPEM and GFC homogenously expressed eye field and RPE markers MITF, PMEL, RPE65, OCC, BEST and ZO-1 by immunofluorescence (Fig. 3B) and displayed functional phagocytosis ability (Fig. 3C) by 90 days (P1), indicating that neither serum nor feeders are required for propagation or differentiation of RPE cells from hPSCs using this protocol. Cell counts indicate that >90 % cells grown with GFC were PMEL positive at day 90, demonstrating the purity of the hPSC-derived RPE culture (Table 1, H9-RPE: 95.35 ± 0.24, n=3; ES4Cl2-RPE: 91.81 ± 3.90, n=3). These results provide a defined system for the generation of mature and mainly homogenous RPE cells for potential use in therapeutics or in circumstances where defined conditions are required.

Transcriptomic profiling indicates close similarity to native human RPE.

Transcriptional profiling was performed to confirm the precise signature associated with the hPSC-derived RPE cells at P0 (day 60, Fig. 4). A total of 5068 genes were up-regulated and 7730 down-regulated in H9-derived RPE cells compared to undifferentiated H9. Supplementary Fig. 2 displays the top 200 differentially expressed genes between H9 and H9-derived RPE cells. Hierarchical clustering confirmed that our H9-derived RPE cells clustered closer to the adult RPE rather than H9 cells (Supplementary Fig. 2).

Discussion

Over 10 years ago, Kawasaki and colleagues demonstrated that co-culturing ESCs with stromal cells could produce RPE-like cells [40]. It was then reported that spontaneous

differentiation of hESCs to RPE-like cells could be achieved by withdrawing bFGF from the culture medium [7]. Both protocols highlighted difficulties in the differentiation process, including low yield, batch variability and phenotypic instability characterised by dedifferentiation of RPE into non-RPE cells. More recent advances have improved upon these early studies and tend to favour more directed approaches to differentiate stem cells into RPE cells, employing the use of specific signalling molecules that recapitulate the developmental events that occur during retinogenesis. A common feature of these more recent differentiation protocols is the two-step approach to differentiating hPSCs to RPE cells. The first step is a deliberate manipulation of the culture medium to promote anterior and neuronal fates, usually facilitated by inhibitors of the Transforming Growth Factor-β and Wnt/beta-catenin-signalling pathways, [8, 14, 21, 22, 41]. Evidence also suggests IGF-1 and bFGF are important for neural induction [42, 43]. In addition, a number of recent studies have demonstrated that other bioactive molecules, including nicotinamide, Activin A, retinoic acid and sonic hedgehog, could also promote RPE differentiation [13, 44]. Although these sequential approaches to RPE differentiation are more defined and directed, they can be complicated, often involving multiple stages of monolayer and three-dimensional culturing, and modifications of media components. Leach *et al* (2015) described a fast differentiation protocol using CHIR99021 to differentiate hESCs to PMEL positive cells in two weeks, followed by enrichment in RPE cells for another 2 weeks (4 weeks in total) [17]. At this stage, the cells showed morphology and pigmentation as well as expression of *PEDF* to suggest functionality of the cells. A further characterization would be needed to evaluate the maturity and homogeneity of these cultures at these time points. Full analysis was performed once cells were enriched, expanded and passaged twice (each passage was performed after 30 days), which would place timing of RPE usage within the same time frame as the protocol we describe here. Using the principles originally described in these multi-step procedures, we

streamlined the existing protocols, directly converting confluent stem cell cultures into RPE cells in a simple and defined one-step approach. By combining Noggin, DKK-1, IGF1 and bFGF within a pro-retinal basal medium, we derived functional RPE cells from hPSCs, which exhibit key features of mature RPE including pigmentation, polygonal morphology, expression of mature markers, functional K^+ channels and the absence of Na^+ currents, and positive phagocytic function. RNA-seq analysis also confirmed a tight resemblance of hPSC-derived RPE cells to primary human adult RPE cells. RPE cells derived from this protocol were capable of repigmentation following enzymatic passaging, which is an important feature, not only for demonstrating the viability of the RPE cells produced using this protocol, but also as a practicality to allow serial expansion of the RPE cells which will be necessary to generate large quantities of cells for drug screening and clinical applications such as cell replacement therapy. Lastly, we demonstrate that the protocol is equally effective using hPSCs in feeder-free conditions and serum-free conditions, enabling this differentiation protocol to be utilised in experiments that require these conditions. Altogether, this one-step differentiation protocol provides a rapid and simplified method of generating a mostly homogenous population of RPE cells from hPSCs.

Acknowledgements

We thank Prof James Thomson (University of Wisconsin) for providing the iPSC line iPS (Foreskin) 4 clone 2, the Lions Eye Donation Service (Melbourne) for providing human donor eyes and the Melbourne Brain Centre's flow Cytometry core facility. We thank Dr Mirella Dottori (University of Melbourne) for providing access to essential equipment for the dissection of POS.

The authors declare no potential conflicts of interest. This work was supported by grants from the NHMRC (1059369), the National Stem Cell Foundation of Australia, the Ophthalmic Research Institute of Australia and the Stafford Fox Medical Foundation. Further support was provided by Australian Postgraduate Award Scholarships (GL, KPG), a NHMRC Career Development Award Fellowship (AP), a NHMRC-CSL Gustav Nossal Postgraduate Research Scholarship (DEC), a NHMRC Early Career Fellowship (AWH), an Australian Research Council (ARC) Future Fellowship (AP, FT140100047), a Cranbourne Fellowship (RCBW), a Gerard Crock Fellowship (KCD), the University of Melbourne and Operational Infrastructure Support from the Victorian Government.

References

1. Davidson, K.C., et al., *Human pluripotent stem cell strategies for age-related macular degeneration.* Optom Vis Sci, 2014. **91**(8): p. 887-93.

2. Kamao, H., et al., *Characterization of human induced pluripotent stem cell-derived retinal pigment epithelium cell sheets aiming for clinical application.* Stem Cell Reports, 2014. **2**(2): p. 205-18.

3. Reardon, S. and D. Cyranoski, *Japan stem-cell trial stirs envy.* Nature, 2014. **513**(7518): p. 287-8.

4. Schwartz, S.D., et al., *Embryonic stem cell trials for macular degeneration: a preliminary report.* Lancet, 2012. **379**(9817): p. 713-20.

5. Schwartz, S.D., et al., *Human embryonic stem cell-derived retinal pigment epithelium in patients with age-related macular degeneration and Stargardt's macular dystrophy: follow-up of two open-label phase 1/2 studies.* Lancet, 2015. **385**(9967): p. 509-16.

6. Leach, L.L. and D.O. Clegg, *Concise Review: Making Stem Cells Retinal: Methods for Deriving Retinal Pigment Epithelium and Implications for Patients With Ocular Disease.* STEM CELLS, 2015. **33**(8): p. 2363-2373.

7. Klimanskaya, I., et al., *Derivation and comparative assessment of retinal pigment epithelium from human embryonic stem cells using transcriptomics.* Cloning Stem Cells, 2004. **6**(3): p. 217-45.

8. Buchholz, D.E., et al., *Rapid and efficient directed differentiation of human pluripotent stem cells into retinal pigmented epithelium.* Stem Cells Transl Med, 2013. **2**(5): p. 384-93.

9. Buchholz, D.E., et al., *Derivation of functional retinal pigmented epithelium from induced pluripotent stem cells.* Stem Cells, 2009. **27**(10): p. 2427-34.

10. Vaajasaari, H., et al., *Toward the defined and xeno-free differentiation of functional human pluripotent stem cell-derived retinal pigment epithelial cells.* Mol Vis, 2011. **17**: p. 558-75.

11. Zahabi, A., et al., *A new efficient protocol for directed differentiation of retinal pigmented epithelial cells from normal and retinal disease induced pluripotent stem cells.* Stem Cells Dev, 2012. **21**(12): p. 2262-72.

12. Zhu, D., et al., *Polarized secretion of PEDF from human embryonic stem cell-derived RPE promotes retinal progenitor cell survival.* Invest Ophthalmol Vis Sci, 2011. **52**(3): p. 1573-85.

13. Idelson, M., et al., *Directed differentiation of human embryonic stem cells into functional retinal pigment epithelium cells.* Cell Stem Cell, 2009. **5**(4): p. 396-408.

14. Osakada, F., et al., *In vitro differentiation of retinal cells from human pluripotent stem cells by small-molecule induction.* Journal of Cell Science, 2009. **122**(17): p. 3169-3179.

15. Reichman, S., et al., *From confluent human iPS cells to self-forming neural retina and retinal pigmented epithelium.* Proceedings of the National Academy of Sciences, 2014. **111**(23): p. 8518-8523.

16. Kuwahara, A., et al., *Generation of a ciliary margin-like stem cell niche from self-organizing human retinal tissue.* Nat Commun, 2015. **6**.

17. Leach, L.L., et al., *Canonical/beta-catenin Wnt pathway activation improves retinal pigmented epithelium derivation from human embryonic stem cells.* Invest Ophthalmol Vis Sci, 2015. **56**(2): p. 1002-13.

18. Zhu, Y., et al., *Three-dimensional neuroepithelial culture from human embryonic stem cells and its use for quantitative conversion to retinal pigment epithelium.* PLoS One, 2013. **8**(1): p. e54552.

19. Nakano, T., et al., *Self-formation of optic cups and storable stratified neural retina from human ESCs.* Cell Stem Cell, 2012. **10**(6): p. 771-85.

20. Cho, M.S., et al., *Generation of retinal pigment epithelial cells from human embryonic stem cell-derived spherical neural masses.* Stem Cell Research, 2012. **9**(2): p. 101-109.

21. Lamba, D.A., et al., *Efficient generation of retinal progenitor cells from human embryonic stem cells.* Proc Natl Acad Sci U S A, 2006. **103**(34): p. 12769-74.

22. Lamba, D.A., et al., *Generation, purification and transplantation of photoreceptors derived from human induced pluripotent stem cells.* PLoS One, 2010. **5**(1): p. e8763.

23. Maminishkis, A., et al., *Confluent monolayers of cultured human fetal retinal pigment epithelium exhibit morphology and physiology of native tissue.* Invest Ophthalmol Vis Sci, 2006. **47**(8): p. 3612-24.

24. Carr, A.J., et al., *Protective effects of human iPS-derived retinal pigment epithelium cell transplantation in the retinal dystrophic rat.* PLoS One, 2009. **4**(12): p. e8152.

25. Yu, J., et al., *Induced Pluripotent Stem Cell Lines Derived from Human Somatic Cells.* Science, 2007. **318**(5858): p. 1917-1920.

26. Thomson, J.A., et al., *Embryonic stem cell lines derived from human blastocysts.* Science, 1998. **282**(5391): p. 1145-7.

27. Molday, R.S., D. Hicks, and L. Molday, *Peripherin. A rim-specific membrane protein of rod outer segment discs.* Invest Ophthalmol Vis Sci, 1987. **28**(1): p. 50-61.

28. Singh, R., et al., *Functional analysis of serially expanded human iPS cell-derived RPE cultures.* Invest Ophthalmol Vis Sci, 2013. **54**(10): p. 6767-78.

29. Stone, A.B., *A simplified method for preparing sucrose gradients.* Biochem J, 1974. **137**(1): p. 117-8.

30. Crombie, D.E., et al., *Characterization of the retinal pigment epithelium in Friedreich ataxia.* Biochemistry and Biophysics Reports, 2015. **4**: p. 141-147.

31. Blankenberg, D., et al., *Manipulation of FASTQ data with Galaxy.* Bioinformatics, 2010. **26**(14): p. 1783-5.

32. Trapnell, C., et al., *Differential gene and transcript expression analysis of RNA-seq experiments with TopHat and Cufflinks.* Nat Protoc, 2012. **7**(3): p. 562-78.

33. Love, M.I., W. Huber, and S. Anders, *Moderated estimation of fold change and dispersion for RNA-seq data with DESeq2.* Genome Biol, 2014. **15**(12): p. 550.

34. Amirpour, N., et al., *Comparing Three Methods of Co-culture of Retinal Pigment Epithelium with Progenitor Cells Derived Human Embryonic Stem Cells.* Int J Prev Med, 2013. **4**(11): p. 1243-50.

35. Gabrielian, K., et al., *In vitro stimulation of retinal pigment epithelium proliferation by taurine.* Curr Eye Res, 1992. **11**(6): p. 481-7.

36. Antonetti, D.A., et al., *Hydrocortisone decreases retinal endothelial cell water and solute flux coincident with increased content and decreased phosphorylation of occludin.* J Neurochem, 2002. **80**(4): p. 667-77.

37. Marsh-Armstrong, N., et al., *Asymmetric growth and development of the Xenopus laevis retina during metamorphosis is controlled by type III deiodinase.* Neuron, 1999. **24**(4): p. 871-8.

38. Rosenthal, R. and O. Strauss, *Investigations of RPE cells of choriodal neovascular membranes from patients with age-related macula degeneration.* Adv Exp Med Biol, 2003. **533**: p. 107-13.

39. Wimmers, S., M.O. Karl, and O. Strauss, *Ion channels in the RPE.* Prog Retin Eye Res, 2007. **26**(3): p. 263-301.

40. Kawasaki, H., et al., *Generation of dopaminergic neurons and pigmented epithelia from primate ES cells by stromal cell-derived inducing activity.* Proc Natl Acad Sci U S A, 2002. **99**(3): p. 1580-5.

41. Meyer, J.S., et al., *Optic vesicle-like structures derived from human pluripotent stem cells facilitate a customized approach to retinal disease treatment.* Stem Cells, 2011. **29**(8): p. 1206-18.

42. Pera, E.M., et al., *Neural and Head Induction by Insulin-like Growth Factor Signals.* Developmental Cell, 2001. **1**(5): p. 655-665.

43. Streit, A., et al., *Initiation of neural induction by FGF signalling before gastrulation.* Nature, 2000. **406**(6791): p. 74-8.

44. Zhang, K., et al., *Direct conversion of human fibroblasts into retinal pigment epithelium-like cells by defined factors.* Protein & Cell, 2014. **5**(1): p. 48-58.

Figure Legends

Figure 1. RPE differentiation. (**A**) Schematic diagram of the culture procedure for RPE differentiation. **(B)** Bright field images of hPSCs cultivated in RPEM with GFC at different time points illustrating changes in cell morphology and emergence of pigmentation at day 20 and day 60. The images shown are from H9 and representative of both cell lines. Scale bars: 100 μm.

Figure 2. Differentiation of hPSCs into functional RPE cells. (**A**) qRT-PCR analysis of *NANOG, OCT4, SIX3, RAX, PAX6, MITF, PMEL, CRALBP, RPE65* for H9- (feeder and feeder-free) and ES4CL2-derived RPE at P0. Human native RPE were used as a positive control for expression of mature RPE cell markers. All data normalized to GAPDH housekeeping gene and respective pluripotent controls (H9 or ES4CL2 respectively) at Day 0. Expression of mature RPE markers in the human RPE was normalised to the ES4CL2 at Day 0. **(B)** Representative immunostaining of RPE cells cultured in RPEM with GFC (P1, n=2 H9-derived RPE, n=2 ES4Cl2-derived RPE) showing expression of MITF, OCC, BEST and ZO-1 in cells merged with DAPI nuclear staining. Scale bars: 50 μm. **(C, D)** Representative phagocytosis assay histograms of ES4CL2-derived and H9-derived RPE at P1 showing fluorescence from internalized FITC-labelled bovine POS after 5-hour incubation. Percentage of internalised POS (green, filled) relative to the untreated (black unfilled, negative control). (**E**) Representative electrophysiological readings of voltage-clamp recordings from RPE cells (ES4CL2-derived, P1), showing the response to changing membrane potential with typical K^+ current, n=19 cells. **(F)** qRT-PCR analysis of pluripotency, eye field and mature RPE markers with increasing enzymatic passage in ES4CL2-derived RPE cells. All data normalized to GAPDH housekeeping gene and pluripotent ES4CL2 control at Day 0. Data expressed are mean ± SEM of three independent

experiments, significance established by (**A**) unpaired t-test or (**F**) unpaired one-way ANOVA using Turkey multiple comparison test, *p<0.05, **p<0.01, ***p<0.001, ****p<0.0001. (**A, F**) Relative quantification: relative expression level of each gene in comparison to its expression level on Day 0 (undifferentiated). **(G)** Heat map of gene expression analysis from H9-derived RPE cells cultivated in RPEM with GFC at P0 (day 60) to P2 (day 120) showing expression changes of pluripotent, eye field and RPE markers. Data normalised to GAPDH and H9 pluripotent cells. Data from two independent experiments.

Figure 3. Feeder-free and serum-free differentiation of hSPCs into RPE cells. (**A**) qRT-PCR analysis of *NANOG*, *OCT4*, *SIX3*, *RAX*, *PAX6*, *MITF*, *PMEL*, *CRALBP*, *RPE65* for H9- and ES4CL2-derived RPE at P0, cultivated with SF-RPEM with GFC without feeders. All data is normalized to GAPDH housekeeping and undifferentiated pluripotent cells at day 0. Data expressed are mean ± SEM of three independent experiments, significance established by unpaired t-test, *p<0.05, **p<0.01, ****p<0.0001. Relative quantification: relative expression level of each gene in comparison to its expression level on Day 0 (undifferentiated). **(B)** Representative immunostaining of RPE cells cultivated in SF-RPEM with GFC without feeders showing expression and localization of MITF, PMEL, RPE65, OCC, BEST and ZO-1 in cells (merged with DAPI nuclear staining) at P1 (n=2 H9-derived RPE, n=2 ES4Cl2-derived RPE). Scale bars: 50 μm. (**C**) Representative phagocytosis assay showing fluorescence from internalized FITC-labelled bovine POS, detected by flow cytometry after 5-hour incubation. Representative histogram of ES4CL2-derived and H9-derived RPE cells at P1 showing the percentage of internalised POS (green, filled) relative to the untreated (black unfilled, negative control).

Supplementary Figure 1. GFC is more robust than basal conditions to induce RPE gene expression. (**A**) Representative image of cells obtained in RPEM only (Basal, top) or with GFC (bottom) at day 60 (P0). (**B, C**) qRT-PCR analysis of *SIX3*, *RAX*, *PAX6*, *MITF*, *PMEL*, *CRALBP* and *RPE65* for (**B**) H9- and (**C**) ES4CL2-derived cells at P0, cultivated with RPEM in the absence or presence of GFC. All data is normalized to GAPDH housekeeping and undifferentiated hPSCs at day 0. Data expressed are mean ± SEM of at least three independent experiments, significance established by two-way ANOVA followed by Sidak multiple comparison test, *$p<0.05$, **$p<0.01$, ***$p<0.001$. Relative quantification: relative expression level of each gene in comparison to its expression level on Day 0 (undifferentiated).

Supplementary Figure 2. Heatmap displaying the top 200 differentially expressed genes between undifferentiated H9 and H9-derived-RPE cells. The corresponding genes in human native adult RPE cells are also displayed. Note the tight cluster of hPSC-derived RPE cells and primary human adult RPE cells.

	PMEL positive cells (% of total cells)
Count 1 (H9)	95.04
Count 2 (H9)	95.20
Count 3 (H9)	95.82
Mean (H9)	95.35 ± 0.24 (n=3)
Count 4 (ES4CL2)	84.06
Count 5 (ES4CL2)	94.95
Count 6 (ES4CL2)	96.41
Mean (Cl2)	91.81 ± 3.90 (n=3)

Table 1: cell count of PMEL positive cells in H9- and CL2-derived RPE cell culture at P1.

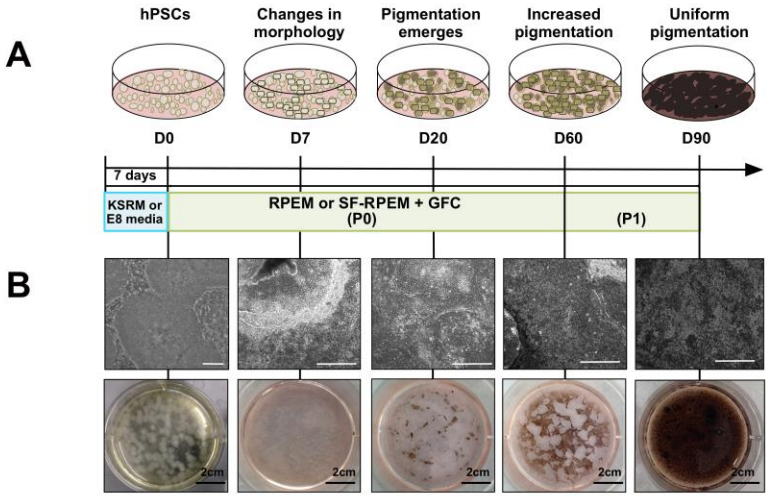
A
hPSCs
Changes in morphology
Pigmentation emerges
Increased pigmentation
Uniform pigmentation
D0
D7
D20
D60
D90
7 days
KSRM or E8 media
RPEM or SF-RPEM + GFC (P0)
(P1)
B
2cm
2cm
2cm
2cm
2cm

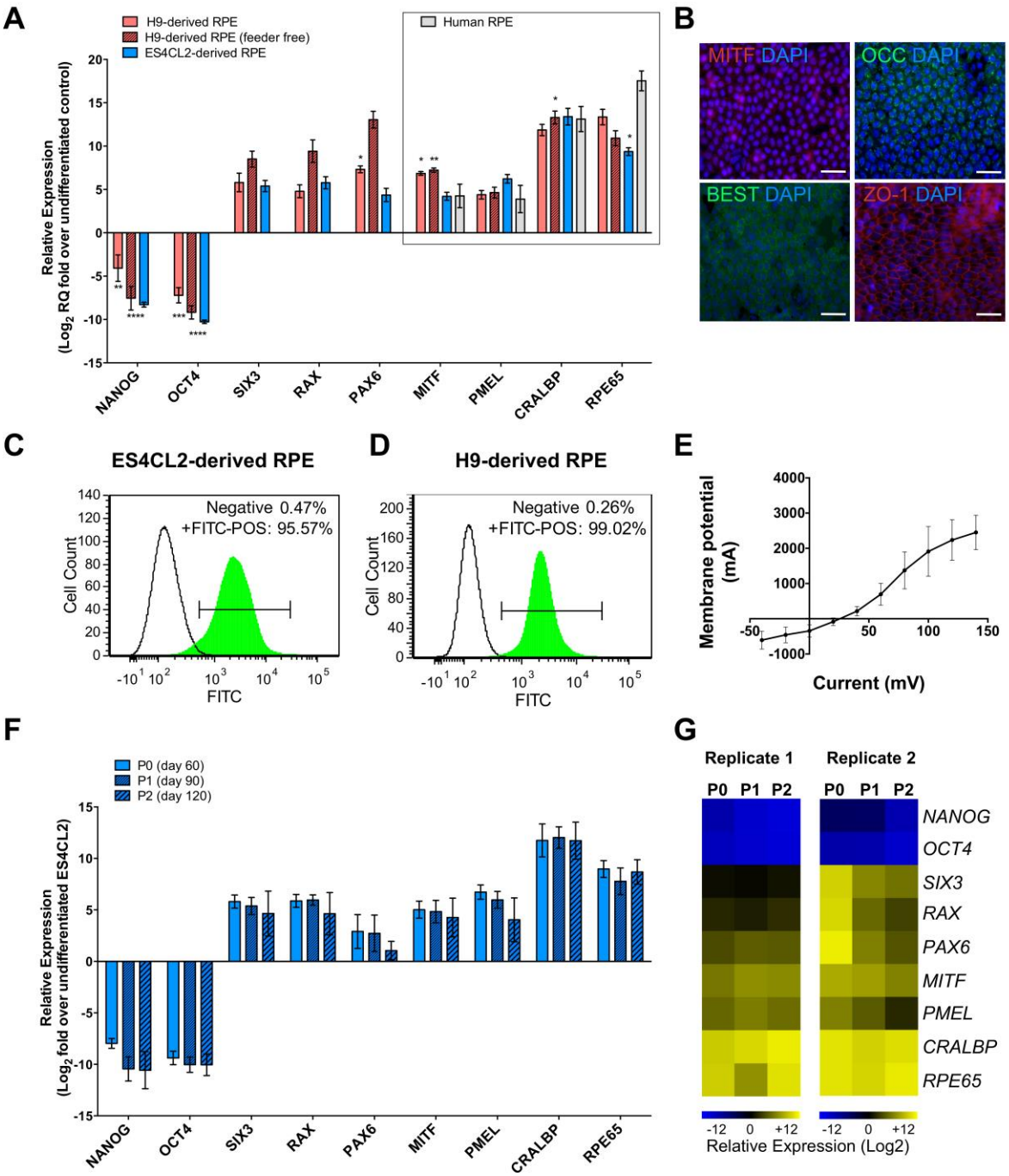
A
H9-derived RPE
H9-derived RPE (feeder free)
ES4CL2-derived RPE
Human RPE
Relative Expression
(Log2 RQ fold over undifferentiated control)
NANOG
OCT4
SIX3
RAX
PAX6
MITF
PMEL
CRALBP
RPE65
B
MITF DAPI
OCC DAPI
BEST DAPI
ZO-1 DAPI
C
ES4CL2-derived RPE
Negative 0.47%
+FITC-POS: 95.57%
Cell Count
FITC
D
H9-derived RPE
Negative 0.26%
+FITC-POS: 99.02%
Cell Count
FITC
E
Membrane potential
(mA)
Current (mV)
F
P0 (day 60)
P1 (day 90)
P2 (day 120)
Relative Expression
(Log2 fold over undifferentiated ES4CL2)
NANOG
OCT4
SIX3
RAX
PAX6
MITF
PMEL
CRALBP
RPE65
G
Replicate 1
Replicate 2
P0 P1 P2
P0 P1 P2
NANOG
OCT4
SIX3
RAX
PAX6
MITF
PMEL
CRALBP
RPE65
-12 0 +12
-12 0 +12
Relative Expression (Log2)

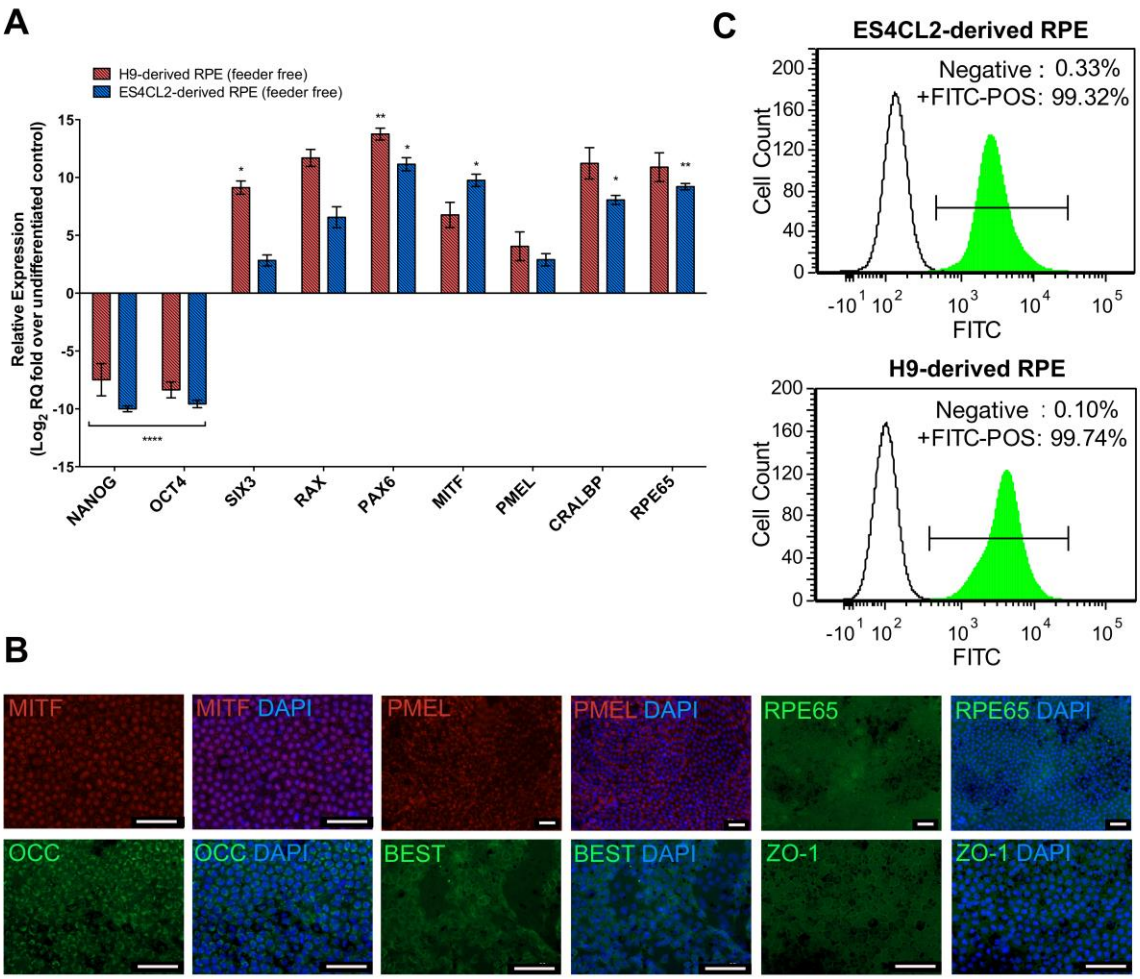
A
H9-derived RPE (feeder free)
ES4CL2-derived RPE (feeder free)
Relative Expression
(Log2 RQ fold over undifferentiated control)
NANOG
OCT4
SIX3
RAX
PAX6
MITF
PMEL
CRALBP
RPE65
C
ES4CL2-derived RPE
Negative : 0.33%
+FITC-POS: 99.32%
Cell Count
FITC
H9-derived RPE
Negative : 0.10%
+FITC-POS: 99.74%
B
MITF
MITF DAPI
PMEL
PMEL DAPI
RPE65
RPE65 DAPI
OCC
OCC DAPI
BEST
BEST DAPI
ZO-1
ZO-1 DAPI